Geomorphology 336 (2019) 1–17

Contents lists available at ScienceDirect

Geomorphology

journal homepage: www.elsevier.com/locate/geomorph

Relicts of mud diapirism of the emerged wedge-top as an indicator of gas hydrates destabilization in the Manila accretionary prism in southern Taiwan (Hengchun Peninsula)

Slawomir Jack Giletycz [a,*], Andrew Tien-Shun Lin [a], Chung-Pai Chang [a,b], J. Bruce H. Shyu [c]

[a] Department of Earth Sciences, National Central University, Chungli 320, Taiwan
[b] Geological Remote Sensing Laboratory, Center for Space and Remote Sensing Research, National Central University, Chungli 320, Taiwan
[c] Department of Geosciences, National Taiwan University, No. 1, Sec. 4, Roosevelt Road, Taipei 106, Taiwan

ARTICLE INFO

Article history:
Received 9 October 2018
Received in revised form 21 March 2019
Accepted 22 March 2019
Available online 25 March 2019

Keywords:
Relict mud volcanoes
Slope basin
Emergence
Southern Taiwan
Hengchun Peninsula

ABSTRACT

Due to oblique collision of the Luzon Volcanic arc and Eurasian passive margin, in Taiwan we observe southward progression of mountain building processes. Consequently, the southernmost tip of Taiwan represents the most recently emerged part of the orogen - the Hengchun Peninsula. The area shows evidence of a trench-slope basin that emerged in the Holocene with landforms that bear submarine characteristics. In the Late Pleistocene, lagoonal sediments blanket the basin, however the deeper deposits (Maanshan Formation) can be found on the surface in several areas. We document that the Maanshan Formation was brought to the surface through upwelling structures—mud diapirs—as a consequence of fast and overpressured sedimentation from the emerging orogen. Although fast erosional processes continuously reorganize the new landscape, we are able to capture relicts of fast eroding inactive mud volcanoes. These unique features are preserved on the surface due to shielding by coral terraces during the shallowing and the lagoonal period of the basin. Stable carbon $\delta^{13}C$ and oxygen $\delta^{18}O$ isotope analysis, performed on samples of carbonate blocks of cold vents collected on the outcrops of the Maanshan Formation, confirm classic seep carbonates origins. We also identify a mud-core anticline below the study area acting as the main source for the mud volcanoes and a possible cause of the uplift of the trench-slope basin. Two multichannel seismic profiles from marine surveys along with a synthesis of several previous surveys helped construct a model of the characteristics of mud diapirism in southeastern offshore Taiwan.

1. Introduction

Mud diapirs and volcanoes are topographic landforms built of unconsolidated fine-grain sediments that are hardly preserved. Mud diapirism is commonly found in fold-and-thrust systems along accretionary zones at convergent plate margins (e.g. Collett et al., 1989; Collett, 1993; Kopf, 2002; Kleinberg et al., 2003). However, it has also been reported in extensional settings (Damuth, 1994; Ivanow et al., 1996; Soto et al., 2010). For example, mud diapirism may indicate periodical or continuous escape of destabilized gas hydrates that migrate up towards the surface due to overpressured material trapped by tectonic compression in the convergent slope basins. On the other hand, several studies describe gravity-driven mud diapir formation due to intrinsic buoyancy contrast and extensional collapse of the thicker orogen (Soto et al., 2010).

In the accretionary prism formation processes rapid sedimentation traps a large quantity of organic matter, producing hydrocarbon gasses that mix with sediment to create slurry medium. This triggers upwards-migration by decreasing pressure of the overlying strata. The migrating gasses form a cold-seep plumbing network and eventually pierce the surface of the seabed, sometimes creating domical structures. After emerging above sea level they are exposed to surface processes and if not capped by coral terraces will cease to exist in a very short time.

The collision between the Eurasian and the Philippine Sea plates produces the Cenozoic Taiwan orogenic complex with a 40–50 km accretionary wedge that forms a fold-thrust belt system between the Manila trench and Luzon volcanic arc (Huang, 2006; Lin et al., 2008) (Fig. 1). The fast-growing narrow orogen induces rapid erosion rates between 3 and 6 mm/yr and large sediment discharge across the island with annual suspended sediment flux up to 88 mm/yr (Dadson et al., 2003). Rapid deposition builds up thick Pliocene to Quaternary sediments that trap a huge amount of organic matter in the Manila accretionary system capable of producing gas hydrates. Gas hydrates form in the upper slope of the prism since their dissociation into free gasses occurs at water depths of less than 650 m (Fig. 1) (Hsu et al., 2013). Intrusions of mud diapirs and mud volcanoes are reported near the shore areas off southwestern Taiwan (Yu and Lu, 1995; Chow et al., 2000;

* Corresponding author.
E-mail address: geojack.slawek@gmail.com (S.J. Giletycz).

https://doi.org/10.1016/j.geomorph.2019.03.022
0169-555X/

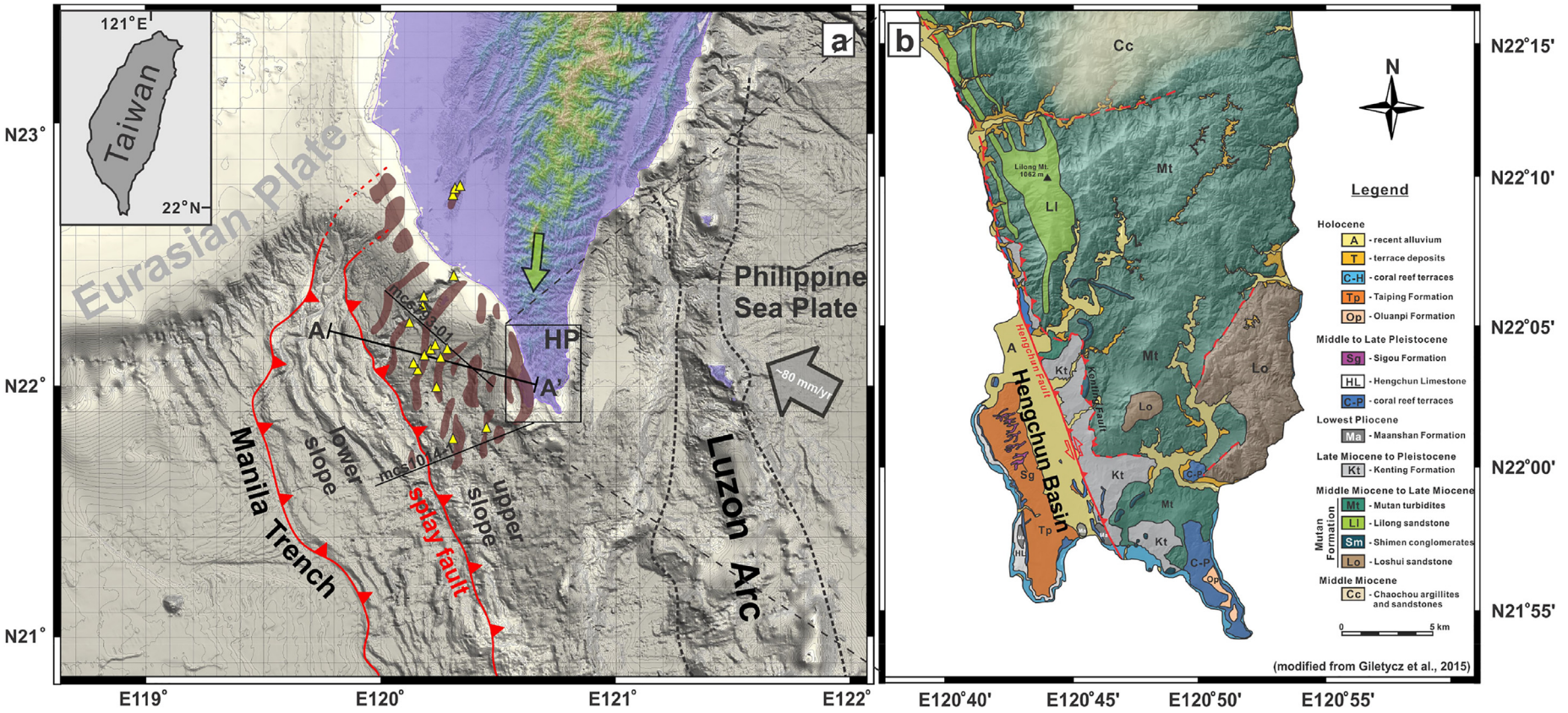

Fig. 1. (a) Tectonic setting of the Taiwan arc-continent collision. The brown areas indicate reported mud diapirs (note areas onshore) (Yu and Lu, 1995; Chow et al., 2000; Chow et al., 2001; Lacombe et al., 2004; Chiang and Yu, 2006; Lin et al., 2009; Chen et al., 2010; Sung et al., 2010; Chiang et al., 2012; Hsu et al., 2013; Chen et al., 2014; Doo et al., 2015). Mud diapirs and volcanoes appear at the overpressured 'upper slope' of the accretionary prism divided from 'lower slope' by a splay fault. The yellow triangles show active mud volcanoes (Chow et al., 2001; Chen et al., 2010; Sung et al., 2010; Chen et al., 2014). The green arrow indicates direction of the progressive emergence of the orogen. The 'HP' rectangle shows the Hengchun Peninsula. Two multichannel seismic reflections transects of profiles shown in Fig. 12a and b. The A–A′ line shows the location of the interpretation profile of the accretionary prism in Fig. 12c; (b) geological map of the Hengchun Peninsula (modified after Giletycz et al., 2015). The Hengchun Basin located to the southwest is separated from the main body of the peninsula by the Hengchun thrust fault with possible sinistral component (red open arrows) (Biq, 1972; Liew and Lin, 1987; Huang et al., 1997; Lin et al., 2008; Giletycz et al., 2017; Deffontaines et al., 2018). (For interpretation of the references to color in this figure legend, the reader is referred to the web version of this article.)

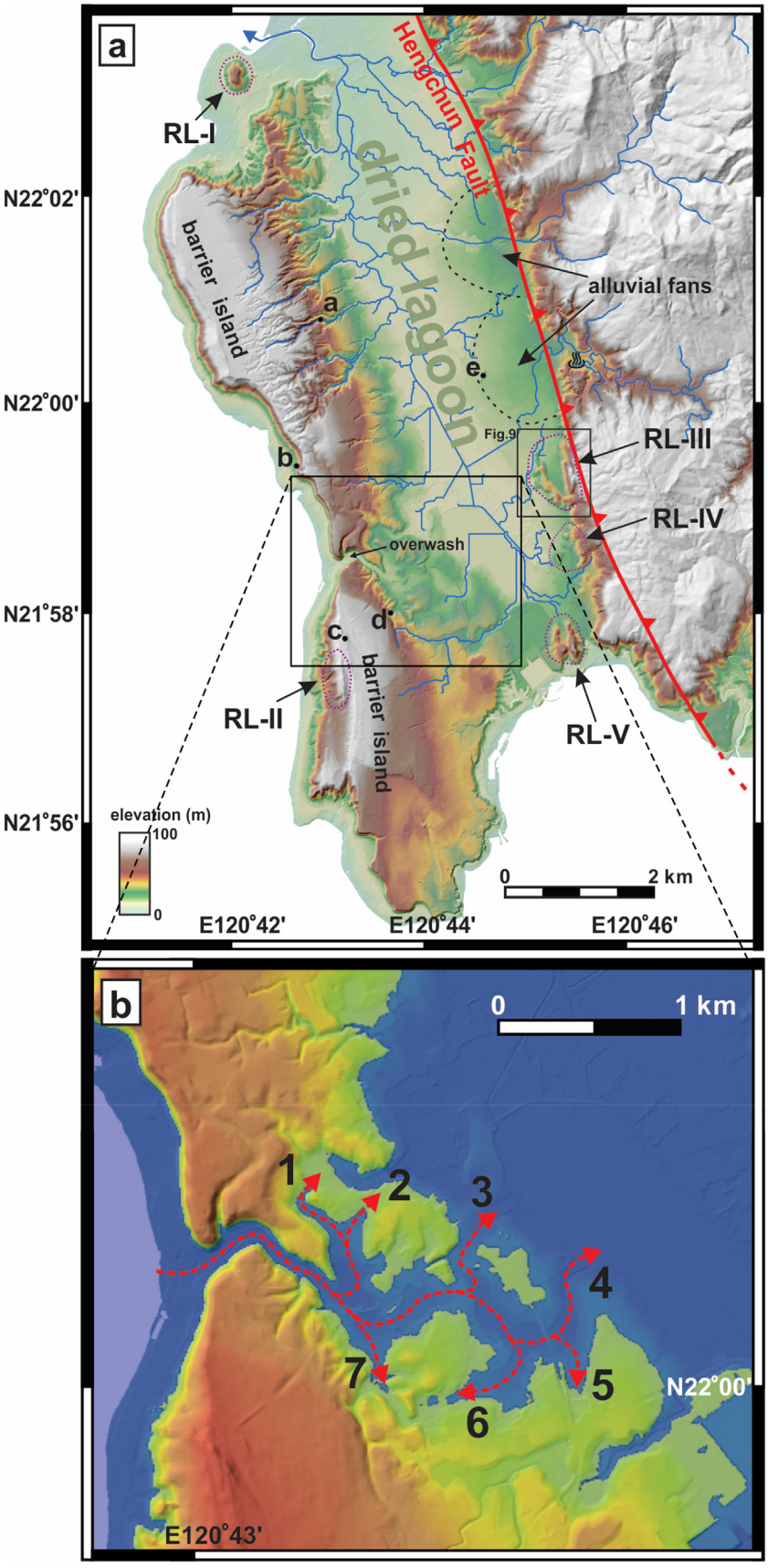

Fig. 2. a) Topographic map of the Hengchun Basin. Barrier islands, wind-gap (overwash) and distributary channels show lagoonal environment before the emergence above the sea level. Note the drainage system draining towards the north, contrary to the progressive, southward emergence of the Hengchun Peninsula. Letters from a) to e) show locations of the photos in Fig. 4. RL symbols from I to V indicate locations of the 'relict landscapes' related to Methane Derived Authigenic Carbonates (MDAC) described in the text; b) flood simulation showing the distributary channels and the overwash between barrier islands (the water raise is 26 m).

Chow et al., 2001; Lacombe et al., 2004; Chiang and Yu, 2006; Lin et al., 2008; Lin et al., 2009; Chen et al., 2010; Sung et al., 2010; Chiang et al., 2012; Chen et al., 2014; Doo et al., 2015; He et al., 2016; Hsu et al., 2018). The number of sites along the Manila accretionary wedge offshore from southwestern Taiwan suggests a strong hydrocarbon potential (e.g. Chuang et al., 2006; Johnson, 2013; Liu et al., 2006; Yang et al., 2006).

Mud diapirs and volcanoes are also found onshore in the Tainan Plain of southwestern Taiwan in the vicinity of the deformation front in the emerged part of the accretionary wedge (Chen and Liu, 2000; Sung et al., 2010; Chao et al., 2011; He et al., 2016).

In this study, we focus on the emerged trench-slope basin of the Manila accretionary prism that indicates relicts of inactive mud volcanoes in the southwestern Hengchun Peninsula, southern Taiwan. Through fieldwork, DEM (digital elevation model) research and stable isotope analyses of collected samples from Methane Derived Authigenic Carbonates (MDAC), we reconstruct a tectonic setting of the emerged basin and correlate our data with the multichannel seismic reflection profiles from two independent marine surveys of R/V Ocean Researcher-1. Additionally, coupling onshore research with offshore profiles of the fold-thrust system, in relation to previous research (Yu and Lu, 1995; Chow et al., 2000; Chow et al., 2001; Lacombe et al., 2004; Chiang and Yu, 2006; Lin et al., 2009; Chen et al., 2010; Chiang et al., 2012; Chen et al., 2014) we synthesize what would help to provide a complete tectonic setting of the mud diapirism in the accretionary wedge from the lower slope to the emerged part of the orogen in southern Taiwan. Here, we addressed two major questions: (1) how surface processes affected the basin's initial conditions after the emergence above sea level, and (2) what is the relationship between mud diapirism and volcanism of the emerged trench-slope basin in the Hengchun Peninsula and the offshore fold-thrust system.

2. Geological and tectonic setting

2.1. Hengchun Peninsula

The collision between the Luzon volcanic arc and the Eurasian passive margin produces a narrow Taiwan orogenic belt formed by the thickening of a weak and young Mesozoic continental basement (e.g. Mouthereau et al., 2013). Thermochronological constraints suggest that the Taiwan collision started ~7 Ma ago and that its current dynamic steady-state was achieved in the last 3 Ma. However, Whipple (2001) argues that the Taiwan orogen is too young to have attained a topographic steady-state. Regardless, the central and southern Taiwan orogen demonstrates southward propagation of the emergence above sea level and successive gradual mountain building processes (Fig. 1a). The southward decrease of elevation and metamorphic grades also indicate a progressive juvenility towards the south. Thus, the Hengchun Peninsula represents the youngest part of the accreted orogen where denudation and landscape reorganization processes have just begun (Ramsey, 2006; Giletycz et al., 2015).

The Hengchun Peninsula is built of Middle Miocene to Holocene formations (Fig. 1b). The main body of the peninsula forms Middle to Late Miocene non-metamorphic or slightly metamorphosed 4000 m thick shales and sandstones (Pelletier and Stephan, 1986) known as the Mutan Formation. They represent sediments deposited on a continental slope of a rifted margin interfingered with deltaic deposits (Lin and Wang, 2001), characterized by a turbiditic and fluxoturbiditic succession of a hemipelagic and pelagic basin plain (Sung and Wang, 1986). Complex and common slumping represents the soft-sediment gravitational deformation of the regional paleoslopes of the fold thrust belt system.

Kenting Formation is the second most common outcropping in the Hengchun Peninsula (Fig. 1b) though the origins of this formation remain the subject of many ongoing debates. Huang et al. (1997) and Chang et al. (2002) suggest the Kenting Formation is a mega-shear zone in which Mutan Formation fault blocks are embedded in a strongly sheared scaly argillaceous matrix containing Neogene and Quaternary microfossils. Consequently, the Kenting Formation is recognized as a tectonic mélange. However, recent studies report evidence of hydrocarbon seepages through that formation (Wang and Mii, 2014) which imply more complex origins. Chaotic deposits interpreted as tectonic mélange or olistostromes composed of unconsolidated mud breccia may indicate the destabilization of gas hydrates (Clari et al., 2004) that likely occurred in the southwestern Hengchun Peninsula (Wang and Mii, 2014).

2.2. Hengchun Basin

In accretionary convergent margins, wedge-tops form subparallel ridges and synclinal-depositional zones (slope basins), which accumulate sediment transported from the upper prism or terrigenous material from an emerged part of an orogen (e.g. Moore and Karig, 1976; Ori and Friend, 1984; Ingersoll, 1988; Okada, 1989; McCrory, 1995; DeCelles and Katherine, 1996; DeCelles, 2012; Bailleul et al., 2013; Nagel et al., 2013). Slope basins typically vary in size from one to several km in width, five to tens of km in length, and several hundred meters to 2–

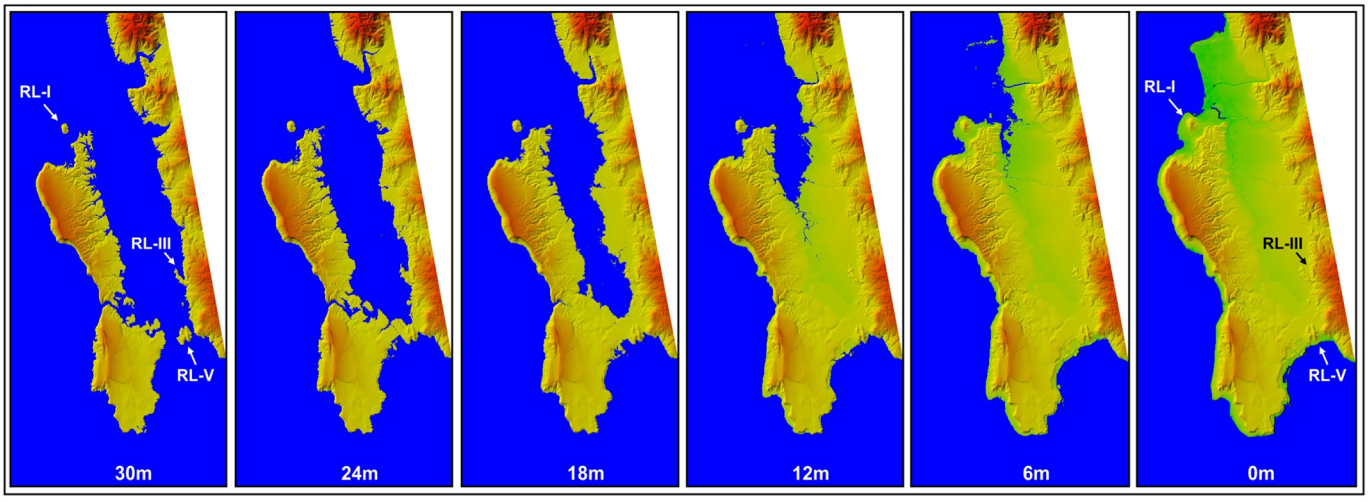

Fig. 3. Flood simulation of the Hengchun Basin. The images show that the central basin of the lagoon was tilted and open at the north where the lagoon was drained out. Barrier islands, overwash and the relict mud volcanoes clearly appear in the images. The rise in water level is indicated at the bottom of each image.

3 km in depth (Moore and Karig, 1976; Okada, 1989; Bailleul et al., 2013).

The southwestern flank of the Hengchun Peninsula represents an elongated 4–5 km wide and 7 km long emerged trench-slope basin, here named as the Hengchun Basin (HB). It is enclosed by the Hengchun Fault to the east and lagoonal barrier islands of sandy Hengchun limestone to the west (Figs. 1b and 2). The HB is filled by Pleistocene clastic sediments of reworked material from the Mutan and Kenting formations (Lin and Wang, 2001) known as the Maanshan Formation. The Maanshan Formation, the lowest unit of the Pliocene to Quaternary marine sediment, is a non-turbiditic, post-mélange formation (Page and Lan, 1983) containing a muddy matrix of Late Miocene nanofossils and Late Pliocene assemblages of mudstone, shale and sandstone. Drilling data indicate its depth to several hundred meters (Chen et al., 2005). However, in a number of sites the lower boundary with the substratum underneath was not reached. By comparison with seismic data of trench-slope basins offshore Taiwan to the west, we estimated the maximum depth of the Maanshan Formation to vary between 1000 and 1300 m. The core data also show that the upper horizon of the Maanshan Formation shallows southward and reaches the surface at the southern part of the trench-slope basin near the south bay of the peninsula (Fig. 1a).

In the Holocene, before a rapid emergence above the sea level (Fig. 3) (Page and Lan, 1983), the trench-slope basin represented a lagoonal environment (Lin and Wang, 2001). Sediments of the shallow-sea near the coast (Lin and Wang, 2001) blanket the Maanshan

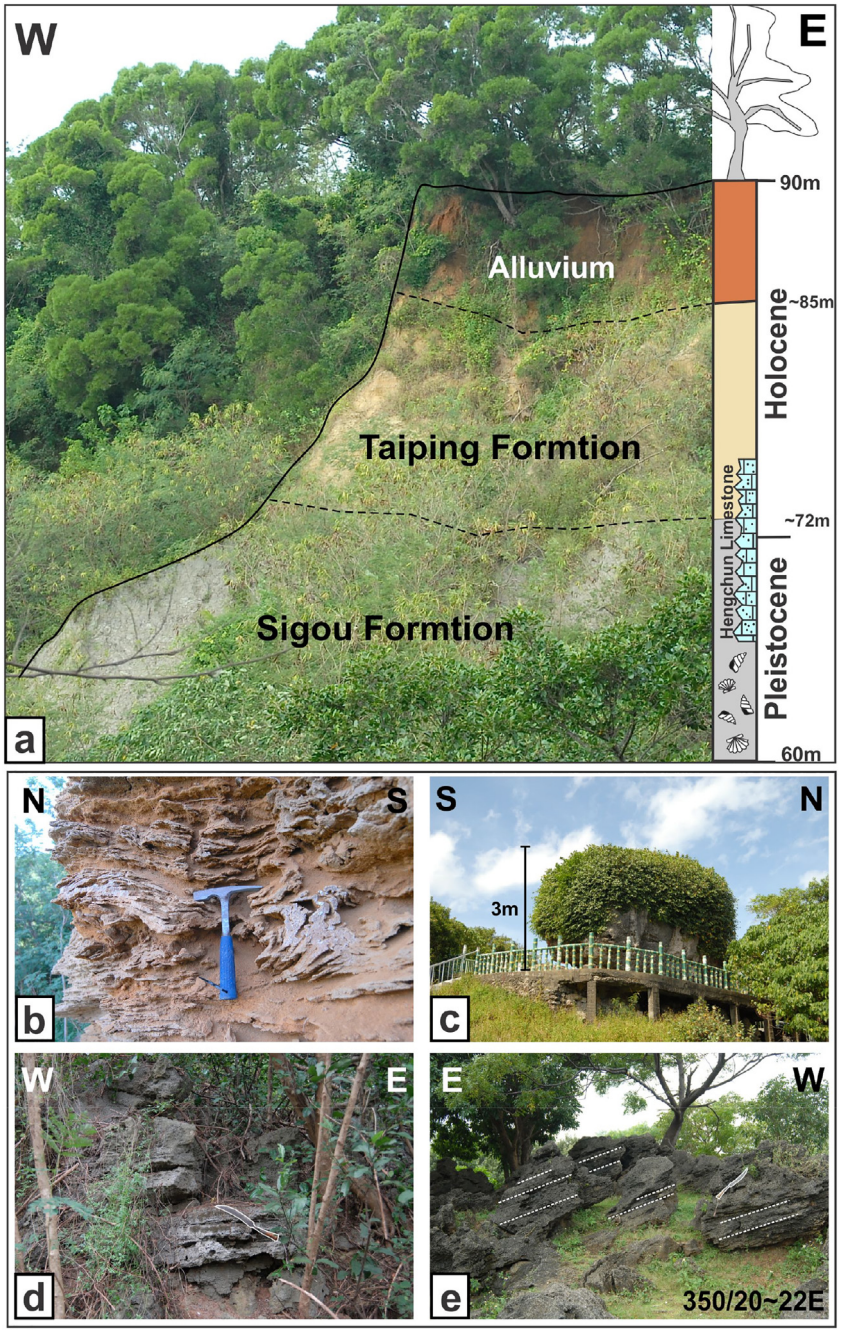

Fig. 4. Lagoonal characteristics of the Hengchun Basin (see location of the sites in Fig. 2). (a) Taiping and Sigou Formations of the HB covered by reddish tropical-weathered alluvium expose their profile in several gullies in the central part of the HB; (b) cross-bedded sandy Hengchun limestone of the barrier island with abundant foraminifers (Cheng and Haung, 1975) and broken shells and corals; (c) coral boulder (in situ) at the top of the uplifted barrier island about 200 m above the sea level presented as a tourist attraction; (d) interfingering Taiping Formation with a coral terrace within the HB; (e) the tilted coral terrace indicates the progressive deformation of the HB.

Formation with two other formations; the Sigou and Taiping Formations. They cover almost the entire trench-slope basin with only a few sites of the outcropping Maanshan Formation visible in the northern, southwestern and southeastern regions, related to the domical landforms of the HB (Fig. 1a). In addition, the Maanshan Formation is linked to the appearance of carbonate cylindrical concentrations that surface at a few outcrops.

The Sigou and Taiping formations characterize lagoonal deposits but differ in developing and emerging stages of the lagoon, respectively (Fig. 4a). Sigou Formation is Pleistocene light greyish sandy and silty sediment, abundant with shells and foraminifera fossils (Yen and Wu, 1986; Chen and Lee, 1990). It can only be found in several deep gullies in the inner part of the Hengchun Basin. Taiping Formation is related to the emergence and post-emergence environment of the lagoon. It is Holocene shallowing-water, yellow to reddish clay and sand conglomerates (Tsan, 1974; Yen and Wu, 1986) that blanket most of the HB and Sigou Formation. In a few areas the Taiping Formation unconformably overlies Sigou Formation and Hengchun Limestone. Both Sigou and Taiping formations are contemporaneous with the barrier islands Hengchun Limestone (Fig. 4b and c).

Within the lagoonal deposits, well-developed Holocene coral terraces interfinger with the Sigou and Taiping Formations across the basin (Fig. 4d). The terraces are tilted eastward 350-015/18-24E, the result of the accretionary wedge mechanisms and basin deformation. To the west, the uplifted barrier islands (Chen et al., 1991) build 200 m cliffs along the western coast of the peninsula. The islands are built of the Holocene, coarse grained, sandy limestone—abundant in shells and broken corals—which is a characteristic of the cross-bedding of the

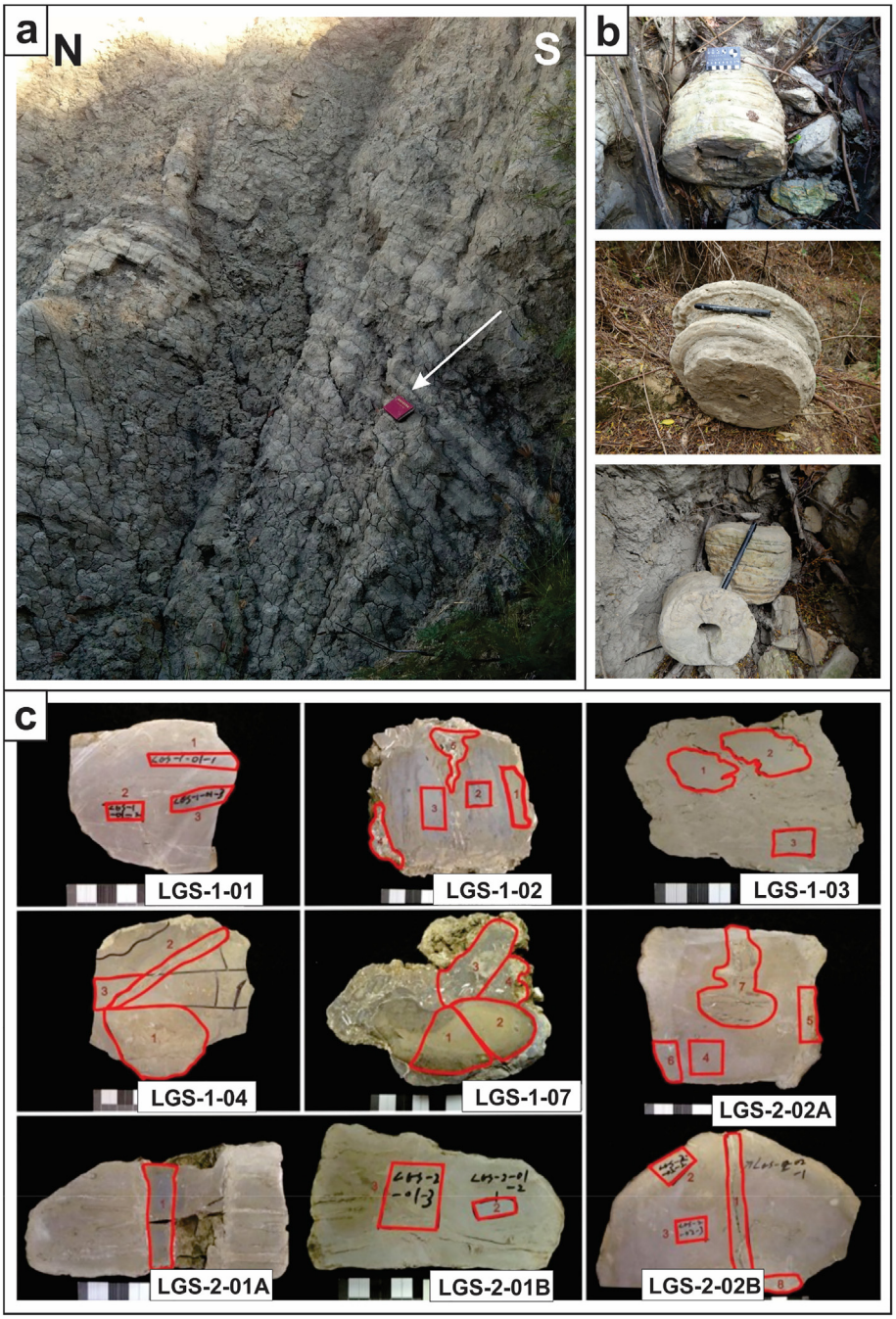

Fig. 5. (a) Maanshan Formation at the western coast below the Hengchun limestone (RL-II, location in the Fig. 2); (b) Methane Derived Authigenic Carbonates (MDAC) of the gas seepage plumbing system; (c) seven samples with acquired ten sub-samples collected from carbonate cylindrical blocks for stable carbon $\delta^{13}C$ and oxygen $\delta^{18}O$ isotope analysis.

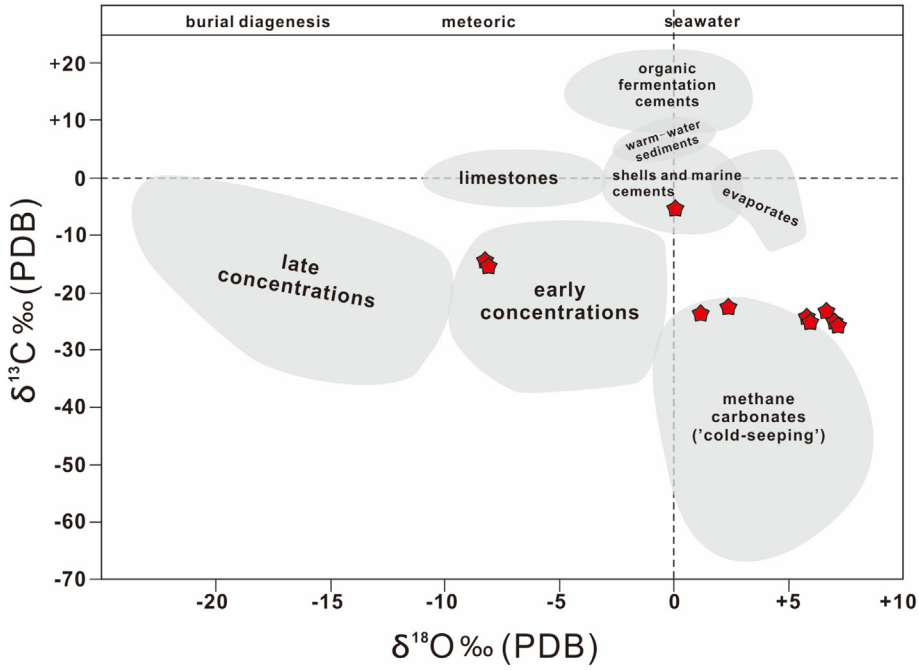

Fig. 6. Results of the ten samples from the southwestern HB on the Phanerozoic cold-seep carbonate plot (Nelson and Smith, 1996; Campbell, 2006).

lagoonal barrier islands (Fig. 4b). They overlay the unconformably tilted Maanshan Formation (Fig. 4e) (Cheng and Haung, 1975).

At present, the juvenile drainage system shows a northwards direction of flow (Fig. 2a). In the central part of the HB, the Lung-Luan Lake could have indicated the remnant of the lagoonal central basin. However, it is an artificial lake likely created during the 'Japanese Period' (1895–1945) and therefore did not record any sedimentology characteristics during lagoon development. For this reason, the lake is discussed no further.

3. Methodology

3.1. Geological mapping and DEM observations

To help understand the geological setting of the emerged slope basin and the landforms within, a detailed geological mapping focused on four areas: (1) formations along the Hengchun Fault to the south; (2) uplifted barrier islands at the western coast of the Hengchun Basin; and (3) gullies in the inner areas of the Hengchun Basin (HB); and (4) dome structures in north and south HB. Furthermore, a significant part of the fieldwork was dedicated to mapping and investigating domes and horse-shoe landforms in the northern and southeastern parts of the basin. Those structures do not represent features from the lagoonal stage of the HB. Therefore, we hypothesize they indicate partially eroded conical mud edifices related to the surfacing of destabilized gas hydrates before the emergence of the basin.

The fieldwork was supported by geomorphological observations using 5–meters scaled DEM (digital elevation model) provided by the Aerial Survey Office of Taiwan Forestry Bureau. Several geomorphological features across the basin surveyed on the DEM directed the field investigation to evidence of lagoonal and diapiric characteristics and demonstrated a relationship between them. In general, DEM observations narrowed our field investigation to particular areas to increase our understanding of the origins of relict landforms in the area.

Table 1
Mineral composition of the chimney carbonate samples from the Maanshan Formation (location in Fig. 4).

Sample	Location	Main mineral composition	$\delta^{13}C/\delta^{12}C$	$\delta^{18}O/\delta^{16}O$
LGS-1-01	N 21°57′40.42″ E 120°43′01.38″	Dolomite, calcite	−24.391	5.596
LGS-1-02	N 21°57′40.14″ E 120°43′00.17″	Calcite, Qtz, dolomite, aragonite	−5.733	0.071
LGS-1-03	N 21°57′39.49″ E 120°42′59.58″	Dolomite, Qtz	−23.704	7.176
LGS-1-04a	N 21°57′39.08″ E 120°42′59.05″	Calcite, Qtz	−14.632	−7.543
LGS-1-04b	N 21°57′39.08″ E 120°42′59.05″	Calcite, Qtz	−15.416	−7.058
LGS-1-07a	N 21°57′39.83″ E 120°42′58.93″	Dolomite, calcite, Qtz	−23.079	1.005
LGS-1-07b	N 21°57′39.83″ E 120°42′58.93″	Calcite, aragonite, Qtz, dolomite	−21.983	2.397
LGS-2-01	N 21°57′38.11″ E 120°43′58.58″	Dolomite, Qtz	−24.607	5.508
LGS-2-02a	N 21°57′36.67″ E 120°42′55.99″	Dolomite, Qtz	−24.225	6.948
LGS-2-02b	N 21°57′36.67″ E 120°42′55.99″	Dolomite, Qtz	−24.654	6.88

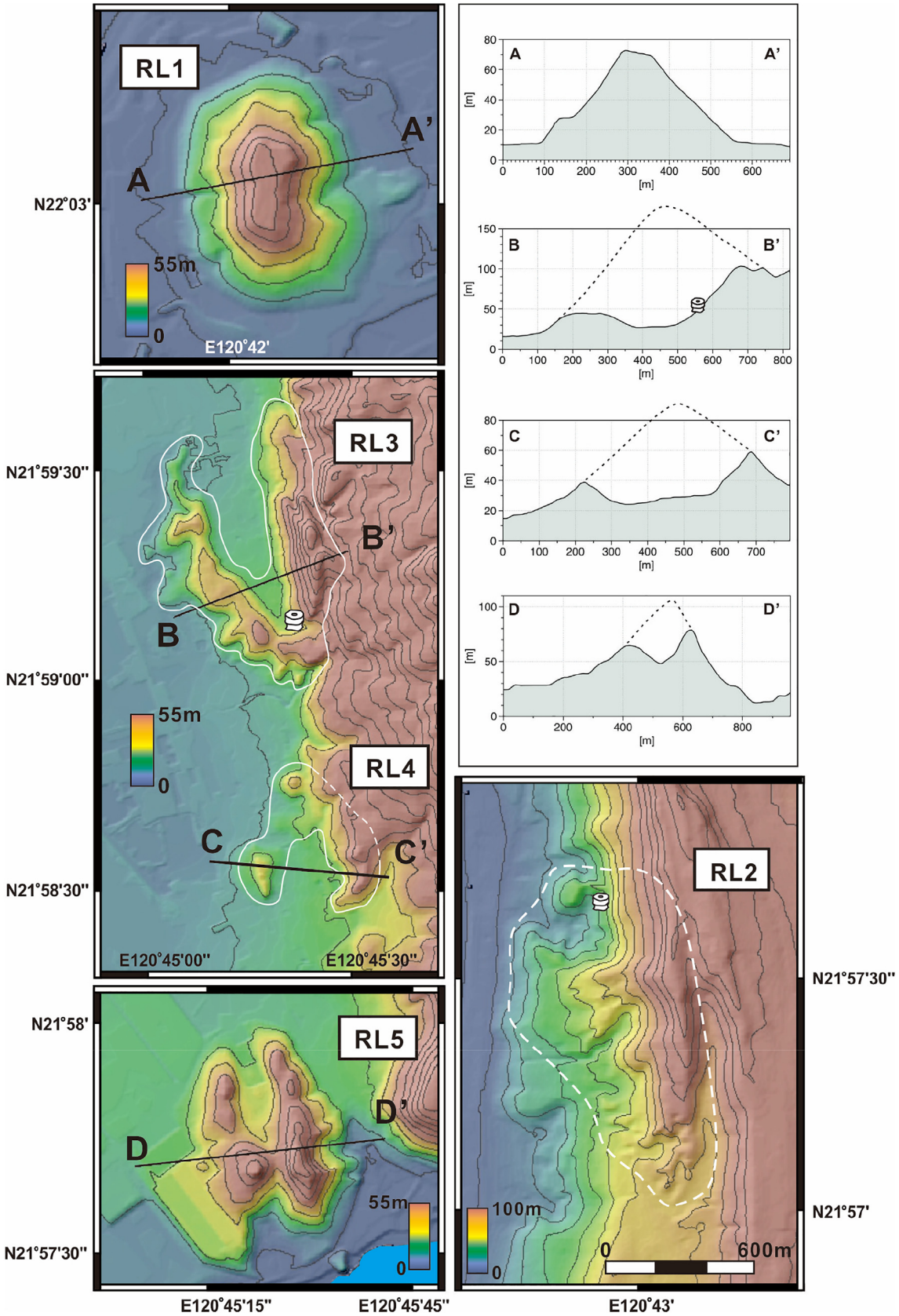

Fig. 7. Horse-shoe and conical landforms related to Methane Derived Authigenic Carbonates (MDAC). Four of them (RL1, RL3, RL4 and RL5) likely indicate mud volcanoes relicts of the HB.

3.2. Stable and gas carbon $\delta^{13}C$, oxygen $\delta^{18}O$ isotope and X-ray diffraction (XRD) analysis

Carbonate cylindrical concentrations were collected from a chaotic assemblage in the Maanshan Formation at the southwestern area of the Hengchun Basin near the coast below the Hengchun limestone and coral terraces. The carbonate blocks appear to represent chimneys of the gas seepage in the Maanshan formation. The aim of this part of the survey was to specify the source of the vents. We used carbon $\delta^{13}C$ and oxygen $\delta^{18}O$ isotope analyses to discriminate the origins of the carbonate mineralization. The analyses were performed on a total of ten samples collected from seven carbonate vents. Stable isotopes of C and O were analyzed in a mass-spectrometer (Thermo-Finnigan MAT253), related to the carbonate standard NBS-19 ($\delta^{13}C = +1.95‰$ and $\delta^{18}O = -2.20‰$ V-PDB) and calibrated to V-PDB (Vienna Pee Dee Belemnite) at National Taiwan University, Taipei, Taiwan. The samples were dissolved in phosphoric acid at 70 °C.

Additionally, the bulk mineral was analyzed using X-ray diffraction (XRD). The samples were analyzed in a D2 PHASER diffractometer (XRD) (Cu Kα radiation, $\lambda = 0.154060$ nm) in the Basin Research Group at National Central University, Taiwan. The intensity of a diffraction peak from a particular mineral is relevant to the abundance of that mineral.

3.3. Correlation to the offshore multichannel seismic reflection profiles

Two multichannel seismic reflection (mcs) profiles were acquired from two cruises of the R/V Ocean Researcher-1 in April 2006 and October 2012, along the upper slope and perpendicular to the accretionary prism, respectively (Fig. 1a). Both cruises were conducted near the shore of southern Taiwan in the South China Sea, though the southern transect reached the lower slope of the accretionary prism to 3100 m. The seismic profiles were processed in the Basin Research Group at National Central University and correlated to the results of our onshore surveys in the Hengchun Basin to build a cross section of the upper accretionary prism including the emerged wedge-top.

4. Results and discussion

4.1. Structural characteristics and MDAC evidence in the Hengchun Basin

Two barrier islands extend along the western HB coast for nearly 10 km. Due to Typhoon Tembin (24 August 2012), well-exposed outcrops of the barrier islands aided investigation of the stratigraphic profile and showed the typical cross-bedding sedimentary structures. The barrier islands are built of Pleistocene sandy limestone with abundant broken mollusks and corals from a surf-zone or swash-zone (Cheng and Haung, 1975) (Fig. 4b). The wind-gap separates the barrier island and indicates remnants of a lagoonal main tidal channel overwash that was active during the emergence of the basin. Average uplift of the barrier islands in the northern and southern parts reaches 150 m and 100 m respectively, with a maximum peak of 217 m above sea level in the north. Along the top of the ridge of the barrier islands, a number of in-situ well-preserved coral boulders indicate the recent marine environment (Fig. 4c). To the east of the wind-gap in the inner area of HB, the overwash developed several distributary channels that are distinct in the DEM and the flood simulation in the Figs. 2b and 3.

In the Holocene, the HB was uplifted closer to the sea surface which resulted in shallow, warm water deposits unconformably covering the tilted Maanshan Formation. A number of sites across the HB reveal characteristics of the emerged lagoon (Figs. 2 and 4). In the central and northern part of the HB, narrow gullies expose the typical 20 m to 30 m of coarse-sand sediments with abundant shells and corals of the Taiping and Sigou Formations, which are blanked by reddish and tropical-weathered recent alluvium (Fig. 4a). The contact between the lagoonal and underlying Maanshan Formations was not found in the field due to dense tropical vegetation and recent thick alluvium cover shielding the bottom of the gullies. However, Cheng and Haung (1975) indicated the unconformity between Maanshan Formation and

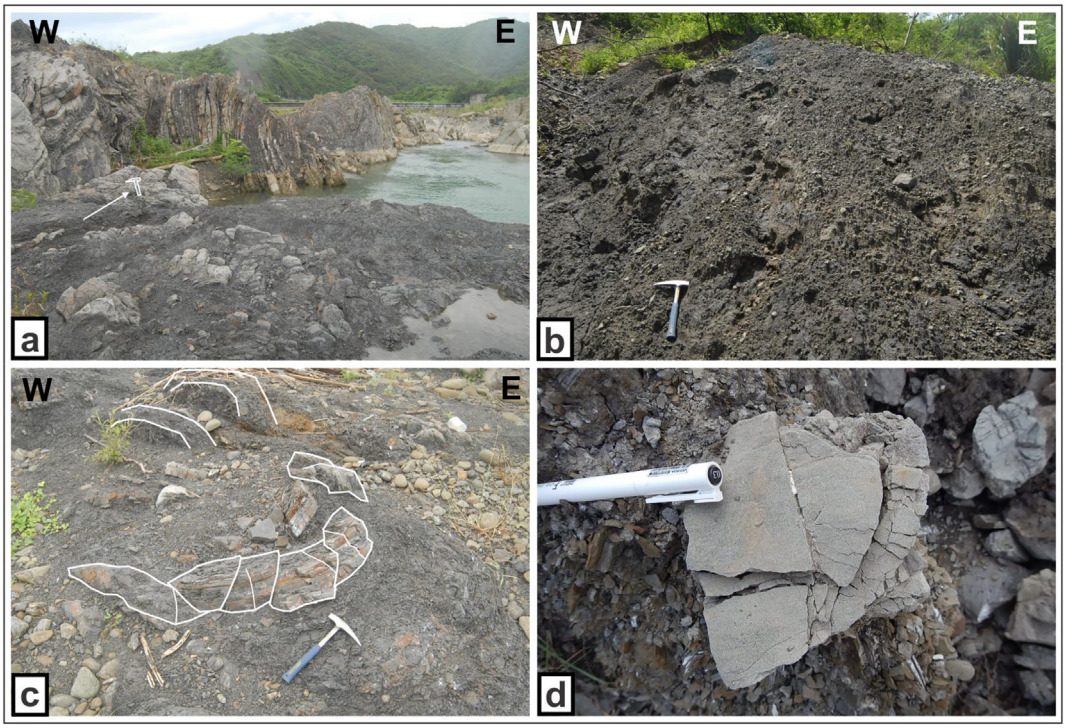

Fig. 8. Breccia and highly sheared material along the Hengchun Fault and in vicinity of the relict landforms indicate hydrocarbon destabilization in the Kenting Formation (Wang and Mii, 2014) and correlate to injections of the overpressured mudstone. Location of the sites: (a) N22°04′45.09″/E120°44′05.97″; (b) N22°00′05.28″/E120°45′28.79″; (c) N22°04′43.35″/E120°44′06.64″; (d) N22°58′01.77″/E120°45′56.34″.

overlying lagoonal sediments. The inner part of the HB characterizes coral terraces interfingering with the Taiping and Sigou Formations (Fig. 4d). Radiocarbon dating of the corals shows higher uplift rates for the western HB than areas at the footwall of the Hengchun Fault (Liew and Lin, 1987; Chen and Liu, 1993).

Although lagoonal deposits blanket the Hengchun Basin, several outcrops of the Maanshan Formation from the slope basin appear on the surface. On the western coast, an outcrop was identified along the southern barrier island cliff exposing contact between mudstones of the Maanshan Formation beneath the Hengchun limestone (Fig. 5a). The mudstone dips 28–35 SE. In a few gullies at the bottom of the outcrop, a large number of MDAC concentrations in cylindrical forms were found ranging from a few cm to 30–35 cm in diameter (Fig. 5b). Since the Maanshan mudstone is an unconsolidated and soft formation,

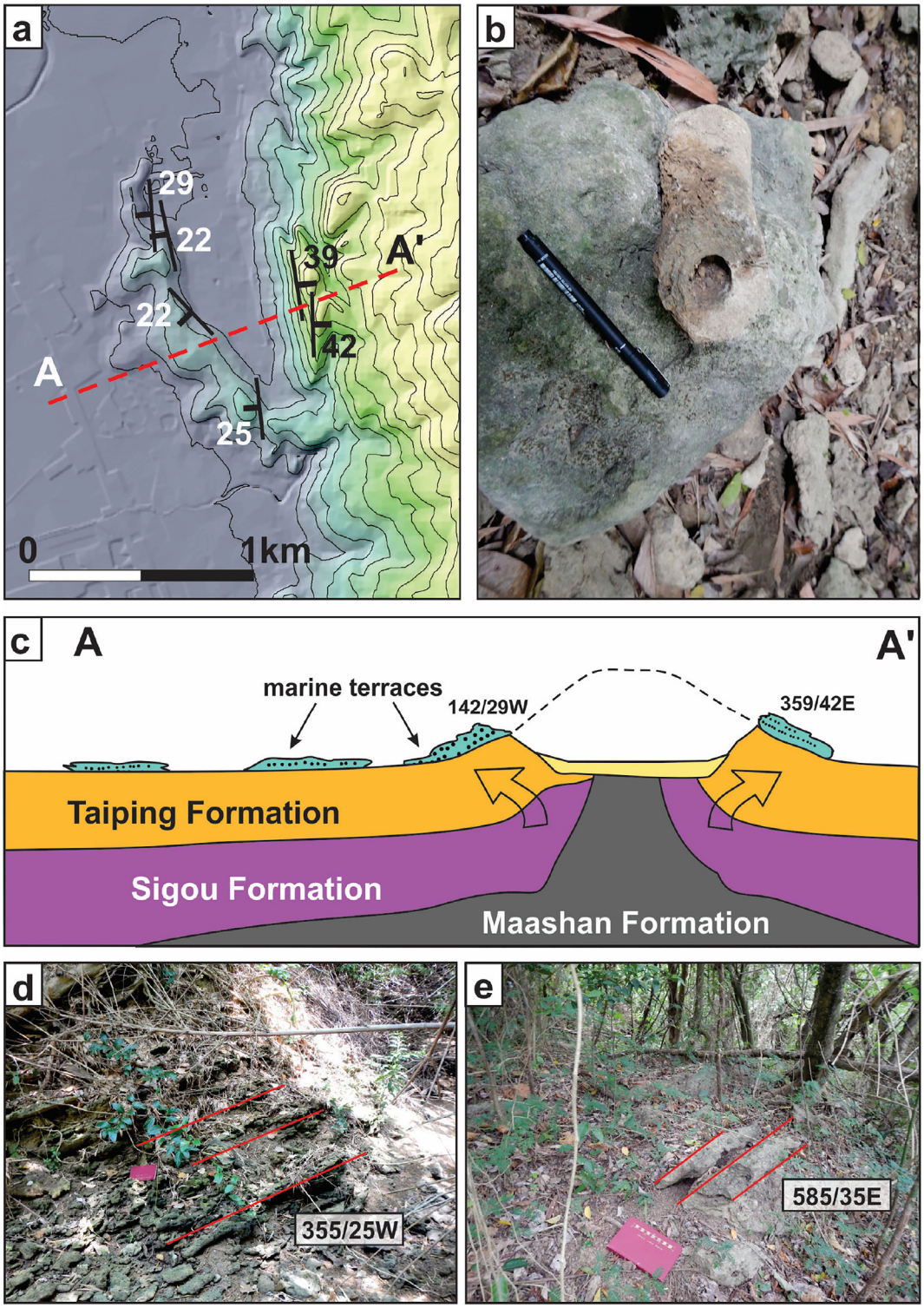

Fig. 9. (a) Horse-shoe landform tilt of the coral terraces indicates a conical uplift. The shape and size of the hill suggest mud volcano origin; (b) carbonate tube of the plumbing system found in the inner part of the landform; (c) interpretative profile across the relict volcano RL-3; (d) and (e) tilt of the coral terraces indicate that the structure was active during the lagoonal stage of the emerging trench-slope basin.

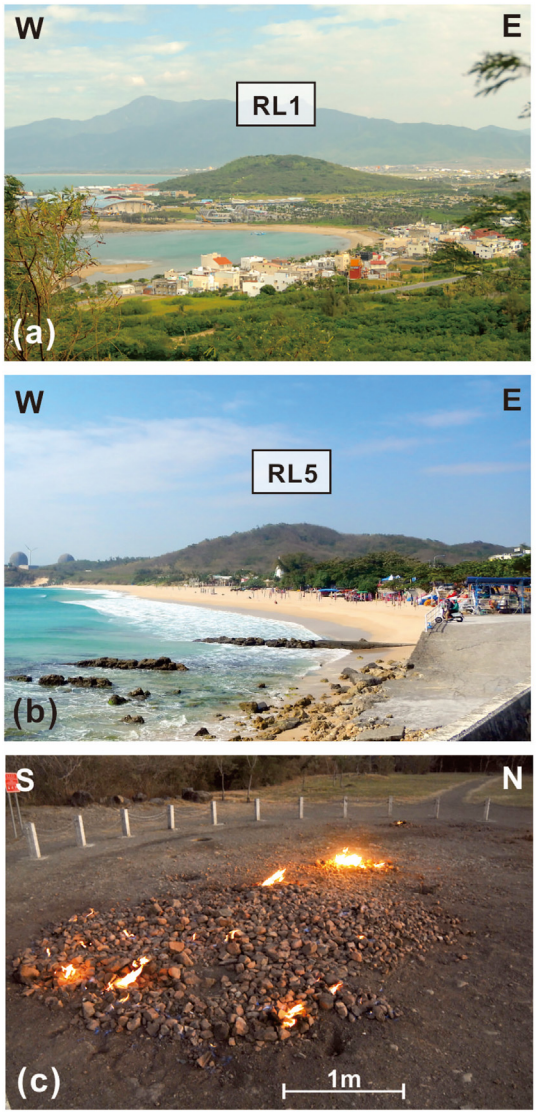

Fig. 10. (a) and (b) photos of the most complete conical-shaped landforms that we interpret as relict mud volcanoes; (c) gas seepage to the north of RV3 (location in Fig. 2).

the blocks were difficult to find in-situ. From seven collected samples, we prepared ten samples for $\delta^{13}C$ and $\delta^{18}O$ isotope analyses (Fig. 5c). The results were plotted on the Phanerozoic cold-seep carbonate graph from Nelson and Smith (1996) and Campbell (2006) to illustrate the origins of the carbonate blocks in the study area (Fig. 6 and Table 1). In seven cases (LGS-1-01, LGS-1-03, LGS-1-07a, LGS-1-07b, LGS-2-01; LGS-2-02a, LGS-2-02b), low $\delta^{13}C$ values between −21 and −25 confirm the methane-related origins as indicated at the summary plot of the Phanerozoic cold-seep carbonates (Fig. 6). Positive values of $\delta^{18}O$ confirmed a seawater environment. Two of the samples showed significantly lower values of $\delta^{18}O$ than typical of cold-seep carbonates. We correlate this to post-depositional dissolution. The $\delta^{13}C$ and $\delta^{18}O$ values demonstrate that carbonate blocks found in the Maanshan Formation result from precipitation of Dolomite, Calcite and Aragonite carbonate cement around transported methane-rich fluids (Table 1). The cylindrical blocks then are remnants of the cold-seep plumbing system caused by overpressured and rapid sedimentation in the unconsolidated sediments and the destabilization of methane gas hydrates of the trench-slope basin.

DEM observations concentrated our fieldwork on several horse-shoe and oval-shaped landforms that represent relict mud volcanoes (Fig. 7) which correlate to the present-day volcanoes offshore of Taiwan (compare with Chen et al., 2014). They are located in the central-eastern and southeastern HB in the vicinity of the Hengchun Fault. Also, one domical hill was located in the northern tip of the HB (Figs. 2, 3, 7 and 9). The landforms do not belong to the lagoonal environment, therefore we postulate that they represent a pre-lagoonal stage of the trench-slope basin. Few of them outcrop Maanshan mudstone, indicating its migration from deeper parts of the HB. Dense tropical vegetation and artificial constructions impeded trenching in the area, however detailed fieldwork brought credible data to support our hypothesis regarding the relict mud volcanoes (Fig. 8).

In the central part of the HB, a 20 m high, elongated arc-shaped hill emerges above the lagoonal Taiping Formation and alluvial deposits (Fig. 9a). It extends in a north-south direction and is covered by a sequence of coral terraces dipping westwards from 22 to 29° (Fig. 9a, c and d). The strike and the dip do not correlate to the main trend of deformation of the HB (compare with Fig. 4e), thus indicating another mechanism of the uplift and tilt. At the same latitude about 300 m to the east, a topographic rise surfaces another set of coral terraces showing contrary dipping 40° eastward. Both features, although distorted by the Hengchun Fault, become apparent at the DEM (Figs. 7 and 9). The coral terraces form a ring shape or horse-shoe structure dipping 'outwards.' Additionally, in the southern part of the area, we found a

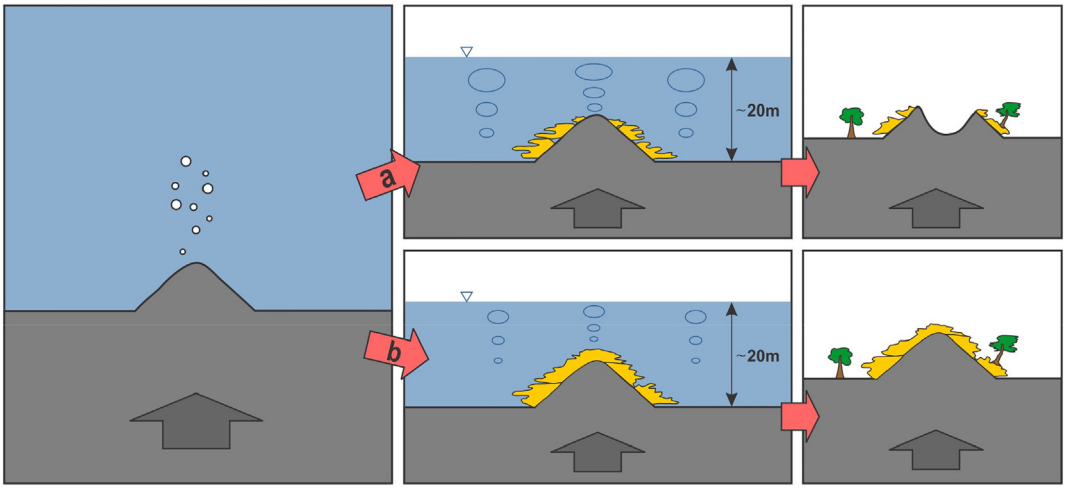

Fig. 11. Two conceptual scenarios for erosional progression of the mud volcano during the emergence above sea level; (a) due to higher sea current energy, the coral terraces partially shield the cone of the volcano, that after the emergence can only armor the slopes, and consequently the inner part is much easier to erode since it is composed of unconsolidated mudstone; (b) lower sea current energy allows the development of thicker coverage of the coral terrace, which after emergence withstands relatively longer erosional processes.

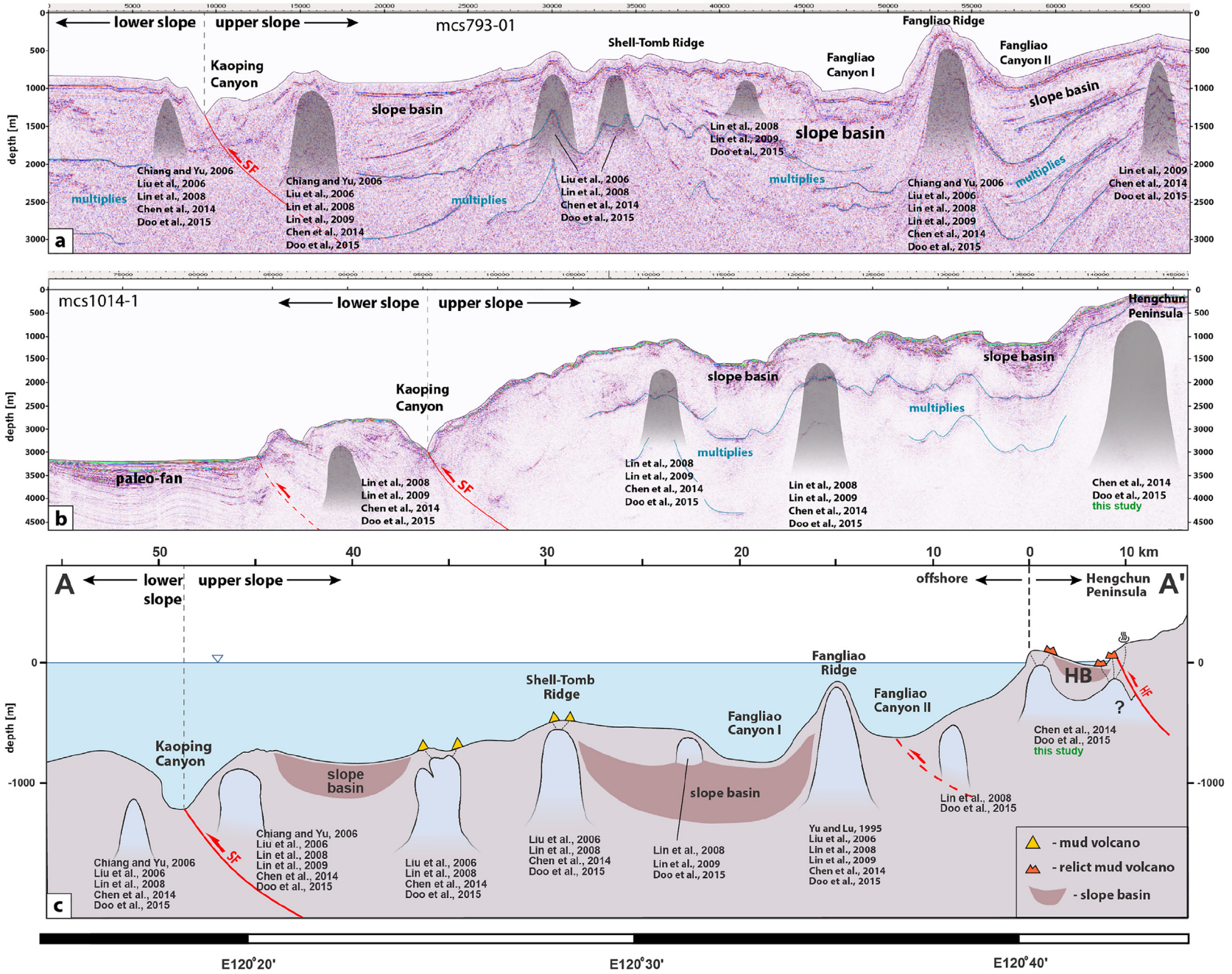

Fig. 12. (a) and (b) Profiles across mud diapirs of the upper part of the accretionary wedge utilizing combined data from two cruises R/V OR-1and previous offshore studies (Chiang and Yu, 2006; Liu et al., 2006; Lin et al., 2008; Lin et al., 2009; Chen et al., 2014; Doo et al., 2015); (c) interpretation of accretionary prism cross section from the lower slope to the on-land survey presented in this work (note different location of the transect than seismic profiles in Fig. 1a).

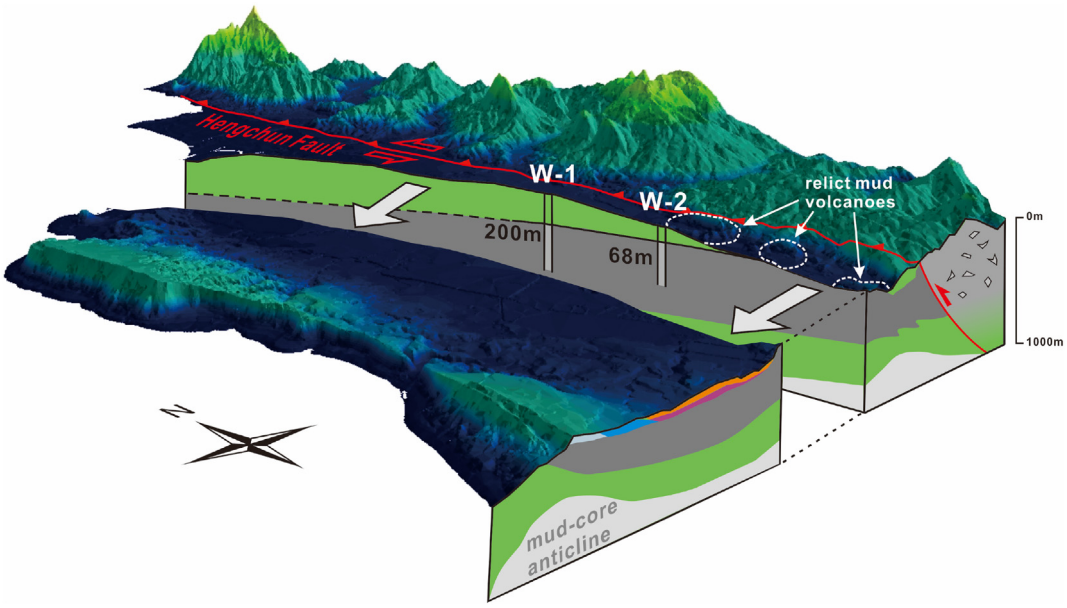

Fig. 13. Well-drilling (W-1 and W-2) along at the footwall of the Hengchun Fault (Chen et al., 2005) reports the Maanshan Formation at 200 m and 68 m in the northern and southern boreholes, respectively. North-dipping Maanshan Formation and relict mud volcanoes at the surface to the south support the concept of the mud diapir below the HB plunging northwards. Detailed explanation of the E-W cross section described in Fig. 15.

carbonate tube at the bottom of the topographic rise (Fig. 9b). We propose the landform represents a relict mud volcano (RL3), which during its activation led to the tilt of the coral terraces 'outwards.' Since we do not find any indication of the activity of the form after the emergence, we suggest that the volcano was active and demised before emergence above sea level and that the main erosional mechanism was related to the marine environments and sea currents (Fig. 9c).

Further south, two similar landforms surface in the vicinity of the Hengchun Fault (RL4 and RL5) suggesting the same mechanism of destabilization gas hydrates (Figs. 7 and 10). RL5 is a well-preserved conic-shaped hill with a partially removed inner part. The landform pattern shows an opening at the northern side (Fig. 7), from where the inner material of the cone was removed (Fig. 11a). However, the field investigation in this area was limited due to restricted access to the

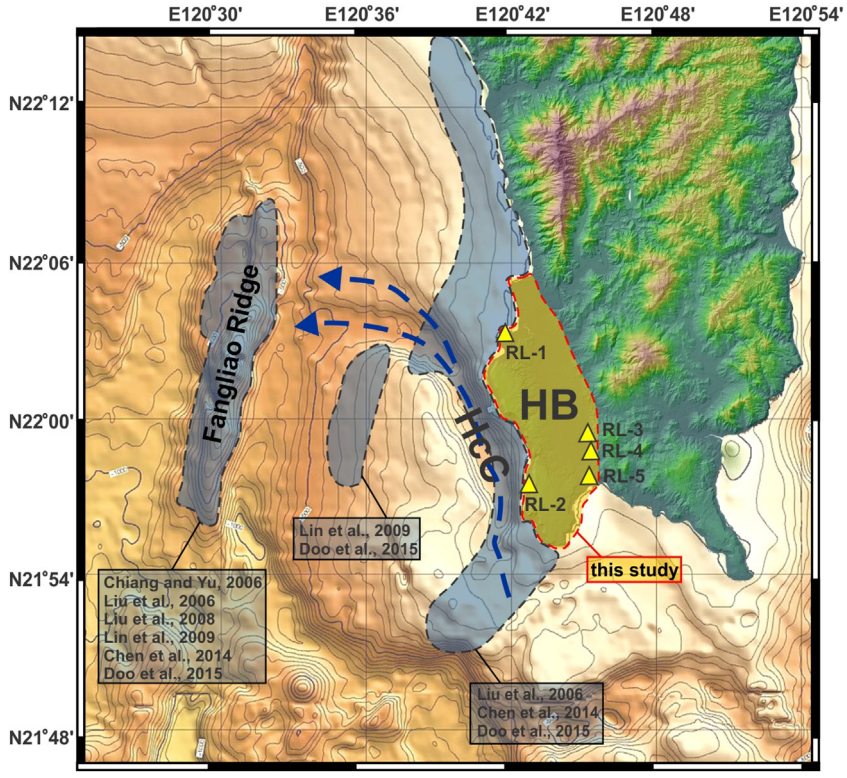

Fig. 14. Model of the mud diapir below the southwestern Hengchun Peninsula from OR-1 mcs profiles, previous marine surveys (Chiang and Yu, 2006; Liu et al., 2006; Lin et al., 2008; Lin et al., 2009; Chen et al., 2014; Doo et al., 2015) and this study. Yellow triangles indicate relict mud volcanoes. Two blue dashed arrows show moats as erosional features due to contour currents along the western coast of the HB. HcC - Hongchai Canyon. (For interpretation of the references to color in this figure legend, the reader is referred to the web version of this article.)

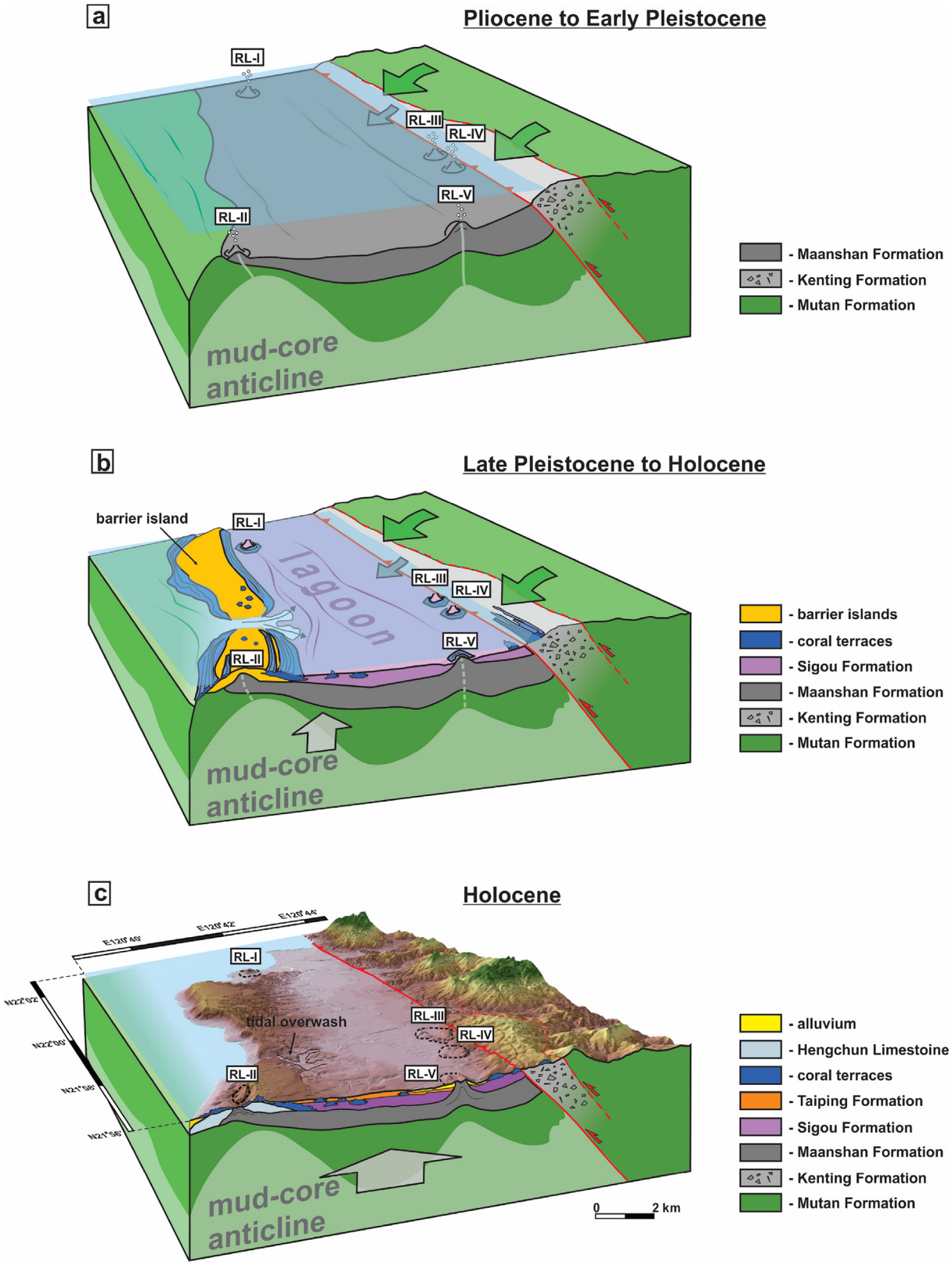

Fig. 15. Evolutionary model of the trench-slope basin of the southwestern Hengchun Peninsula. (a) Trench-slope basin stage. Rapid sedimentation from erosion emerged the Mutan Formation and Kenting Mélange by depositing material with large amounts of organic matter. The overpressure of the produced gas hydrates leads to mud diapirism; (b) lagoon stage. An emerging basin changes the environment to warmer and shallow water. Sediment of the same source then fills the already lagoonal basin blocked by barrier islands to the west; (c) onshore stage. The emerged basin exposes landforms of preexisting mud volcanoes and lagoonal features as tidal overwash, barrier islands. However, continuous erosion progressively erodes the mud volcanoes leaving oval-shaped relicts covered by more resistant coral terraces. Alluvial deposits cover the lagoon, though the deformation of the basin still remains active.

Maanshan Nuclear Power Plant III facility where RL5 is located. RL4 is densely overgrown with vegetation and characterizes a low-elevated landform with an advanced stage of erosion and coverage of alluvial deposits (Fig. 7). Therefore, our survey on those two landforms—RL4 and RL5—is mostly based on DEM observations.

In the northern part of the HB, a landform RL1 represents the most complete conic-shaped feature in the research area. Its large and small diameters reach 500 m and 400 m, respectively (Figs. 2 and 7) and it is composed of mudstone of the Maanshan Formation with a thick cover of coral terraces reaching several meters thick. We relate the preservation of the RL1 cone to thick shielding by the coral terraces that preserved the entire volcano from erosional processes (Fig. 11b).

In general, three conical landforms (RL1, RL3 and RL5) characterize the same erosional mechanism that effected in longitudinal direction and progressed the structures inwards. We relate this pattern to the south-to-north trending Kuroshio Pacific sea current (Qui, 2001). Although the current itself flows in about 50 km east of Taiwan, it still partially intrudes into the South China Sea through the Luzon Strait (Nan et al., 2015; Seo et al., 2015; Chang et al., 2018) and directly affects temperature, salinity and transport of the sediment. In Fig. 14, clear erosional moats west of the HB offshore indicate active erosion due to the counter current (Hernández-Molina et al., 2008). During the uplift and closure to the surface of the HB, the shallowing current incasing its energy became the main erosional factor affecting the emerging new landforms that resulted in the longitudinal removal of the landforms.

In total, we have located five sites that indicate presence of destabilization gas hydrates (Figs. 2 and 8). The identified characteristics of destabilization of gas hydrates are as follows: (1) in three locations (RL1, RL2, RL5), the Maanshan Formation was reported at the surface; (2) in two (RL2 and RL3), the carbonate tubes confirm methane-related origins; (3) in four (RL1, RL3, RL4 and RL5), the topography and horseshoe tilt of coral terraces indicate relict cones. Fieldwork and DEM observations do not assess RL2 as a mud volcano, thus it may represent remnants of the cold-seep plumbing network. Additionally, a potential relict RL-4 is under advanced erosional processes that obscure its origins. Therefore, we do not consider this landform in our mud volcanism record.

The appearance of gas seepage and mud volcanoes on the surface argues for destabilization of gas hydrates during the trench-slope basin development. Comparing to residual gravity surveys by Doo et al. (2015) the HB shows strong correlation with the offshore mud diapirs in the upper slope of the prism (Fig. 12). Residual positive gravity anomaly indicates high possibility of the mud diapir beneath the basin. Also, the north-dipping horizon of the Maanshan formation in Chen et al. (2005) markedly corresponds to the relict mud volcanoes in the southern HB (Fig. 13). Consequently, based on seismic profile observations and previous surveys (Lin et al., 2009; Chen et al., 2014; Doo et al., 2015) we postulate that the mud diapir reported west offshore further extends eastward under the trench-slope basin (Fig. 14), representing an additional mechanism for recent and observed short wavelength deformation.

4.2. Conceptual evolutionary model of the southwestern Hengchun Peninsula

The appearance of the cold-seep plumbing network and conical hills over the HB with the correlation of seismic profiles offshore west allows us to frame the development and growth of the HB from the depositional to the present stage of emerged dried lagoon with its initial erosional processes (Fig. 15):

1) During Pliocene to Early Pleistocene, fold and thrust belt processes developed a trench-slope basin at the wedge-top at the southern emerging Taiwan orogen (Fig. 15a). As a result of reworked material from Mutan and Kenting Formations, the Maanshan Formation was deposited in the shallow, relatively close to the source basin (Page and Lan, 1983; Lin and Wang, 2001). Rapid sedimentation from fast uplift of the wedge-top with organic matter produced large amounts of gas hydrates. Compression caused mud diapirism and consequently led to the piercing of the basin to the surface.
2) In Late Pleistocene, a continuous accretion of the prism raised the basin close to the surface developing shallow depositional environment. The barrier islands grew about 5 km offshore from the coast initiating lagoon conditions over the basin with typical lagoonal features, such as (1) tidal overwash, (2) warm water sediments, and (3) coral terraces (Fig. 15b). The Mutan and Kenting Formations remained chief sources for the lagoonal deposition. Coral terraces covered conical landforms, barrier islands and other areas along the Hengchun Fault. Volcanoes did not reveal any further activity. Due to the fracturing of the carbonate shield of the relict landforms, the intrusion of the Kuroshio current initiated erosional processes in S-N direction. Since the lagoon remained open in the northern and southern part, the current was able to flow and carried out the eroded material substructing the carbonate layer. However, the relict volcanoes armored by coral terraces preserved as onshore partially eroded landforms. Only one relict landform to the north of the HB preserved as a fully-grown cone.
3) Early Holocene until the present. The lagoon dried out, moving the coastline 5–6 km to the west (Figs. 15c and 3). The overwash discontinued transporting the tidal currents into the HB leaving a 1 km wide wind-gap. Simultaneously, the first drainage system developed with an outlet at the northern coast of the HB (Fig. 2a). The Holocene alluvial sedimentation—including alluvial fans from the main body of the peninsula (Figs. 1 and 2)—covers the lagoonal deposits, outcropping them only in several gullies, especially in the northern part of the HB. Several relict mud volcanoes remain on the surface. At the same time, the advancing uplift of the HB emerges succeeding coral terraces above the sea level at the rates of 2–3 mm/yr (Chen and Liu, 1993).

5. Conclusions

In this work we present a complete profile of the southern orogen from the offshore parts to the emerged wedge-top of the accretionary prism. The Hengchun Basin (HB) represents a typical setting of a trench-slope basin of the accretionary wedges filled by close-to-the-source, shallow sediments. The low complexity of the basin suggests that it was developed in the upper zone of the accretionary prism, however synsedimentary thrusting across the HB is expected. The tilt of the coral terraces over the HB indicates a continuous deformation of the basin during its emergence above sea level in the Holocene. One of the significant findings in our study is that the Maanshan Formation outcrops at the surface through mud diapirism. Stable carbon $\delta^{13}C$ and oxygen $\delta^{18}O$ isotope analysis confirm the typical cold-seep carbonates processes in the area. Topographic and geologic evidence aid the interpretation of the mud volcanoes in the Hengchun Basin. Therefore we suspect that Kenting Formation is also associated with the occurrence of cold-seep and mud diapirism processes, and not only as the tectonic mélange encompassing the eastern boundary of the trench-slope basin. However, fully understanding the role of mud diapirism over formations at the hanging wall of the Hengchun Fault requires further work.

Acknowledgments

We would like to thank Guan-Linag for assistance during the stable isotope analysis of the carbonate tubes. We also thank anonymous reviewers for vital advice and suggestions to improve our manuscript.

This work was granted by MOST (104-2116-M-008-022; 102-2628-M-002-007-MY3; 104-2811-M-002-047; and 105-2811-M-002-030).

References

Bailleul, J., Chanier, F., Ferriere, J., Robin, C., Nicol, A., Mahieux, G., Gorini, C., Caron, V., 2013. Neogene evolution of lower trench-slope basin and wedge development in the central Hikurangi subduction margin, New Zealand. Tectonophysics 591, 152–174.

Biq, C.-C., 1972. Dual-trench structure in the Taiwan-Luzon region. Geological Society of China 15, 65–75.

Campbell, K.A., 2006. Hydrocarbon seep and hydrothermal vent paleoenvironments and paleontology: past developments and future research directions. Palaeogeogr. Palaeoclimatol. Palaeoecol. 232, 362–407.

Chang, C.-P., Angelier, J., Lee, T.-G., Huang, C., 2002. From continental margin extension to collision orogen: structural development and tectonic rotation of the Hengchun peninsula, southern Taiwan. Tectonophysics 361, 61–82.

Chang, M.-H., Jan, S., Mensah, V., Andres, M., Rainville, L., Yang, Y.J., Cheng, Y.H., 2018. Zonal migration and transport variations of the Kuroshio east of Taiwan induced by eddy impingements. Deep-Sea Res. I 131, 1–15.

Chao, H.-C., You, C.-F., Wang, B.-S., Chung, C.-H., Huang, K.-F., 2011. Boron isotopic composition of mud volcano fluids: implications for fluid migration in shallow subduction zones. Earth Planet. Sci. Lett. 305, 32–44.

Chen, Y.-G., Liu, T.-K., 1993. Holocene radiocarbon dates in Hengchun Peninsula and their neotectonic implications. J. Geol. Soc. China 36 (4), 457–479.

Chen, Y.-G., Liu, T.-K., 2000. Holocene uplift and subsidence along an active tectonic margin south-western Taiwan. Quat. Sci. Rev. 19 (9), 923–930.

Chen, W.-S., Lee, W.-C., 1990. Reconsideration of the stratigraphy on the Western Hengchun Hill. Ti-Chih (Geology) 10 (2), 127–140.

Chen, H.-W., Wu, L.-C., Huang, C.-Y., Koichiro, M., 1991. Late Pleistocene molluscan paleoecology of lagoon deposits of the Szekou Formation, Hengchun Peninsula, Southern Taiwan. Proceedings of the Geological Society of China 34 (1), 57–87.

Chen, W.-S., Lee, W.-C., Hunag, N.-W., Yen, I.-C., Yang, C.-C., Yang, H.-C., Chen, Y.-C., Sung, S.-H., 2005. Characteristics of accretionary prism of Hengchun Peninsula, southern Taiwan: Holocene activity of the Hengchun Fault. Western Pacific Earth Sciences 5, 129–154.

Chen, S.-C., Hsu, S.-K., Tsai, C.-H., Ku, C.-Y., Yeh, Y.-C., Wang, Y., 2010. Gas seepage, pockmarks and mud volcanoes in the near shore of SW Taiwan. Mar. Geophys. Res. 31, 133–147.

Chen, S.-C., Hsu, S.-K., Wang, Y., Chung, S.-H., Chen, P.-C., Tsai, C.-H., Liu, C.-S., Lin, H.-S., Lee, Y.-W., 2014. Distribution and characters of the mud diapirs and mud volcanoes off the southwest Taiwan. J. Asian Earth Sci. 92, 201–214.

Cheng, Y.-M., Haung, C.-Y., 1975. Biostratigraphic study in the west Hengchun Hill. Acta Geol. Taiwan. 18, 49–59.

Chiang, C.-S., Yu, H.-S., 2006. Morphotectonics and incision of the Kaoping submarine canyon, SW Taiwan orogenic wedge. Geomorphology 80, 199–213.

Chiang, C.-S., Yu, H.-S., Noda, A., TuZino, T., Su, C.-C., 2012. Avulsion of the Fangliao submarine canyon off southwestern Taiwan as revealed by morphological analysis and numerical simulation. Geomorphology 177–178, 26–37.

Chow, J., Lee, J.-S., Sun, R., Liu, C.-S., Lundberg, N., 2000. Characteristics of the bottom simulating reflectors near mud diapirs: offshore southwestern Taiwan. Geo-Mar. Lett. 20, 3–9.

Chow, J., Lee, J.-S., Liu, C.-S., Lee, B.-D., Watkins, J.S., 2001. A submarine canyon as the cause of a mud volcano - Liuchieuyu Island in Taiwan. Mar. Geol. 176, 55–63.

Chuang, P.-C., Yang, T.S., Lin, S., Lee, H.-F., Lan, T.F., Hong, W.-L., Liu, C.-S., Chen, J.-C., Wang, Y., 2006. Extremely high methane concentration in bottom water and cored sediments from offshore southwestern Taiwan. Terr. Atmos. Ocean. Sci. 17 (4), 903–920.

Clari, P., Cavagna, S., Martire, L., Hunziker, J., 2004. A Miocene mud volcano and its plumbing system: a chaotic complex revisited (Monferrato, NW Italy). J. Sediment. Res. 74 (5), 662–676.

Collett, T.S., 1993. Natural gas hydrates of the Prudhoe Bay and Kuparuk River area, North Slope, Alaska. AAPG Bull. 77, 793–812.

Collett, T.S., Bird, K.J., Kvenvolden, K.A., Magoon, L.B., 1989. Gas hydrates of Arctic Alaska. AAPG Bull. 73, 345–346.

Dadson, J.D., Hovius, N., Chen, H., Dade, W.B., Hsieh, M.-L., Willet, S.D., Hu, J.-C., Horng, M.-J., Chen, M.-C., Stark, C.P., Lague, D., Lin, J.-C., 2003. Links between erosion, runoff, variability and seismicity on the Taiwan orogen. Nature 426, 648–651.

Damuth, J.E., 1994. Neogene gravity tectonics and depositional processes on the deep Niger delta continental margin. Mar. Pet. Geol. 11 (3), 321–346.

DeCelles, P.G., Katherine, K.A., 1996. Foreland basin systems. Basin Res. 8, 105–123.

DeCelles, P.G., 2012. Foreland Basin Systems Revisited: Variations in Response toTectonic Settings, Tectonics of Sedimentary Basins. John Wiley & Sons, Ltd., pp. 405–426.

Deffontaines, B., Chang, K.-J., Champenois, J., Lin, K.-C., Lee, C.-T., Chen, R.-F., Hu, J.-C., Magalhaes, S., 2018. Active tectonics of the onshore Hengchun Fault using UAS DSM combined with ALOS PS-InSAR time series (southern Taiwan). Nat. Hazards Earth Syst. Sci. 18, 829–845.

Doo, W.-B., Hsu, S.-K., Liao, C.-L., Chen, S.-C., Tsai, C.-H., Lin, J.-Y., Huang, Y.-P., Huang, Y.-S., Chiu, S.-D., Ma, Y.-F., 2015. Gravity anomalies of the active mud diapirs off southwest Taiwan. Geophys. J. Int. 203, 2089–2098.

Giletycz, S.J., Loget, N., Chang, C.-P., Moutherau, F., 2015. Transient fluvial landscape and preservation of low-relief terrains in an emerging orogen: example from Hengchun Peninsula, Taiwan. Geomorphology 231, 169–181.

Giletycz, S.J., Chang, C.-P., Lin, A.T.-S., Ching, K.-E., Shyu, J. Bruce H., 2017. Improved alignment of the Hengchun Fault (southern Taiwan) based on fieldwork, structure-from-motion, shallow drilling, and levelling data. Tectonophysics 721, 435–447.

He, J., Wang, S., Zhang, W., Yan, W., Lu, Z., 2016. Characteristics of mud diapirs and mud volcanoes and their relationship to oil and gas migration and accumulation in a marginal basin of the northern South China Sea. Environ. Earth Sci. 75, 1122.

Hernández-Molina, F.J., Llave, E., Stow, D.A.V., 2008. In: Rebesco, M., Camerlenghi, A. (Eds.), Continental Slope Contourites, Contourites (Developments in Sedimentology, Volume 60). Elsevier B.V., Great Britain, pp. 379–408.

Hsu, S.-K., Wang, S.-Y., Liao, Y.-C., Yang, T.-F., Jan, S., Lin, J.-Y., Chen, S.-C., 2013. Tide-modulated gas emitions and tremors off SW Taiwan. Earth Planet. Sci. Lett. 369–370, 98–107.

Hsu, S.-K., Lin, S.-S., Wang, S.-Y., Tsai, C.-H., Doo, W.-B., Chen, S.-C., Lin, J.-Y., Yeh, Y.-C., Wang, H.-F., Su, C.-W., 2018. Seabed gas emissions and submarine landslides off SW Taiwan. Terr. Atmos. Ocean. Sci. 29 (1), 7–15.

Huang, C.-Y., 2006. Foraminiferal paleoecology of a late Pleistocene lagoonal sequence of the Szekou formation in the Hengchun Peninsula, Southern Taiwan. Proceedings of the Geological Society of China 33, 181–206, 1988.

Huang, C.-Y., Wu, W.-Y., Chang, C.-P., Tsao, S., Yuan, P.-B., Lin, C.-W., Xia, K.-Y., 1997. Tectonic evolution of accretionary prism in the arc-continent collision terrane of Taiwan. Tectonophysics 281, 31–51.

Ingersoll, R.V., 1988. Tectonics of sedimentary basins. Geol. Soc. Am. Bull. 100, 1704–1719.

Ivanow, M.K., Limonov, A.F., van Weering, T.C.E., 1996. Comparative characteristics of the Black Sea and Mediterranean Ridge mud volcanoes. Mar. Geol. 132, 253–271.

Johnson, N., 2013. Small state hydrocarbon exploration in the South China Sea. Canadian Naval Review 9 (2).

Kleinberg, R.L., Flaum, C., Griffin, D.D., Brewer, P.G., Malby, G.E., Peltzer, E.T., Yesionowski, J.P., 2003. Deep sea NMR: methane hydrate growth habit in porous media and its relationship ti hydraulic permeability, deposit accumulation, and submarine slope stability. J. Geophys. Res. 108 (B10), 2508. https://doi.org/10.1029/2003JB002389.

Kopf, A.J., 2002. Significance of mud volcanism. Rev. Geophys. 20 (2).

Lacombe, O., Angelier, J., Mouthereau, F., Chu, H.-T., Deffontaines, B., Lee, J.-C., Rocher, M., Chen, R.-F., Siame, L., 2004. The Liuchiu Hsu island offshore SW Taiwan: tectonic versus diapiric anticline development and comparisons with onshore structures. Compt. Rendus Geosci. 336, 815–825.

Liew, P.-M., Lin, C.-F., 1987. Holocene tectonic activity of the Hengchun Peninsula as evidenced by the deformation of marine terraces. Mem. Geol. Soc. China 9, 241–259.

Lin, S.-B., Wang, Y.-R., 2001. Clay minerals in the rock formations on the Hengchun Peninsula, Southern Taiwan, and their tectonic implications. Eastern Pacific Earth Sciences 1 (2), 157–174.

Lin, T.-S., Liu, Char-Shine, Lin, Che-Chuan, Schnurle, Philippe, Chen, Guan-Yu, Liao, Wei-Zhi, Teng, Louis S., Chuang, Hui-Ju, Wu, Ming-Shyan, 2008. Tectonic features associated with the overriding of an accretionary wedge on top of a rifted continental margin: an example from Taiwan. Mar. Geol. 255, 186–203.

Lin, A.T.-S., Yao, B., Hsu, S.-K., Liu, C.-S., Huang, C.-Y., 2009. Tectonic features of the incipient arc-continent collision zone of Taiwan: implications for seismicity. Tectonophysics 479, 28–42.

Liu, C.-S., Schnurle, P., Wnag, Y., Chung, S.-H., Chen, S.-C., Hsiuan, T.-H., 2006. Distribution and characters of gas hydrate offshore of the southwestern Taiwan. Terr. Atmos. Ocean. Sci. 17 (4), 615–644.

McCrory, P.A., 1995. Evolution of a trench-slope basin within the Cascadia subduction margin: the Neogene Humboldt Basin California. Sedimentology 42 (2), 223–247.

Moore, G.F., Karig, D.E., 1976. Development of sedimentary basins on the lower trench slope. Geology 4 (11), 693–697.

Mouthereau, F., Watts, A.B., Burov, E., 2013. Structure of orogenic belts controlled by lithosphere age. Nature Geoscience Letters 6, 785–789.

Nagel, S., Castelltort, S., Wetzel, A., Willett, S.D., Mouthereau, F., Lin, A.T.-S., 2013. Sedimentology and foreland basin paleogeography during Taiwan arc continent collision. J. Asian Earth Sci. 62, 180–204.

Nan, F., Xue, H., Yu, F., 2015. Kuroshio intrusion in the South China Sea: a review. Prog. Oceanogr. 137, 314–333.

Nelson, C.S., Smith, A.M., 1996. Stable oxygen and carbon isotope compositional fields for skeletal and diagenetic components in New Zealand Cenozoic nontropical carbonate sediments and limestones: a synthesis and review. N. Z. J. Geol. Geophys. 39, 93–107.

Okada, H., 1989. Anatomy of trench-slope basins: examples from the Nankai Trough. Palaeogeogr. Palaeoclimatol. Palaeoecol. 71, 3–13.

Ori, G.G., Friend, P.F., 1984. Sedimentary basins formed and carried piggyback on active thrust sheets. Geology 12, 475–478.

Page, B.M., Lan, C.-Y., 1983. The Kenting mélange and its record of tectonic events. Mem. Geol. Soc. China 5 (227), 248.

Pelletier, B., Stephan, J.F., 1986. Middle Miocene obduction and late Miocene beginning of collision registered in the Hengchun Peninsula: geodynamics implications for the evolution of Taiwan. Mem. Geol. Soc. China 7, 301–324.

Qui, B., 2001. Kuroshio and Oyashio Currents. University of Hawaii at Manoa Academic Press, pp. 1413–1425.

Ramsey, L.A., 2006. Topographic Evolution of the Emerging Mountain Belts. Universuty of Cambridge (PhD Thesis).

Seo, G.-H., Choi, B.-J., Cho, Y.-K., Kim, Y.H., Kim, S., 2015. Evaluation of a regional reanalysis system for the East Asian Marginal Seas based on the ensemble Kalman filter. Ocean Science Journal 50, 29–48.

Soto, J.I., Fermin, F._i., Talukder, A., 2010. Miocene shale tectonics in the northern Alboran Sea (western Mediterranean). The American Association of Petroleum Geologists 93, 1–26.

Sung, Q., Wang, Y., 1986. Sedimentary environments of the Miocene sediments in the Hengchun Peninsula and their tectonic implication. Mem. Geol. Soc. China 7, 325–340.

Sung, Q.-C., Chang, H.-C., Liu, H.-C., Chen, Y.-C., 2010. Mud volcanoes along the Chishan fault in Southwestern Taiwan: a release bend model. Geomorphology 118, 188–198.

Tsan, S.-F., 1974. Stratigraphy and structure of the Hengchun Peninsula, with special reference to a Miocene olistostrome. Bulletin of the Geological Survey of Taiwan 24, 100–108.

Wang, S.-W., Mii, H.-S., 2014. Stable isotope evidence for hydrocarbon seepages in the Kenting Mélange at Baoli, Hengchun Peninsula, Taiwan. Collection and Research 27, 95–106.
Whipple, K.X., 2001. Fluvial landscape response time: how plausible is steady-state denudation? Am. J. Sci. 301, 313–325.
Yang, T.-F., Chuang, P.-C., Lin, S., Chen, J.-C., Wnag, Y., Chung, S.-H., 2006. Methane venting in gas hydrate potential area offshore of SW Taiwan: evidence of gas analysis of water column samples. Terr. Atmos. Ocean. Sci. 17 (4), 933–950.
Yen, T.-P., Wu, C.-Y., 1986. The Piocene and younger formations in the southern part of the Hegnchun Peninsula. Ti-Chis (Geology) 7 (1), 1–10.
Yu, H.-S., Lu, J.-C., 1995. Development of the shale diapir-controlled Fangliao Canyon on the continental slope off southwestern Taiwan. J. SE Asian Earth Sci. 11 (4), 265–276.